

# Physalin B attenuates liver fibrosis via suppressing LAP2 $\alpha$ -HDAC1 mediated deacetylation of GLI1 and hepatic stellate cell activation

Xiaoyun Zhu<sup>1</sup>, Shengtao Ye<sup>1</sup>, Jie Li<sup>1</sup>, Meihui Zhang<sup>1</sup>, Yanqiu Zhang<sup>1</sup>, Yingrong Leng<sup>1</sup>, Ting Yang<sup>1</sup>, xinlin Chen<sup>1</sup>, Jianguang Luo<sup>1</sup>, Hao Zhang<sup>1</sup>, and LY Kong<sup>1</sup>

<sup>1</sup>China Pharmaceutical University

December 2, 2020

## Abstract

**Background and Purpose:** Liver fibrosis is one of the leading causes of morbidity and mortality worldwide of which no acceptable therapy exists. Accumulating evidence supports that glioma-associated oncogene homologue 1 (GLI1) is a potentially important therapeutic target for liver fibrosis. This study investigates the antifibrotic activities and potential mechanisms of Physalin B (PB), a natural Solanaceae compound. **Experimental Approach:** Mice subjected to CCl<sub>4</sub> challenge and bile duct ligation were used to study the antifibrotic effects of PB in vivo. Mouse primary hepatic stellate cells (pHSCs) and human HSC line LX-2 also served as an in vitro liver fibrosis model. Liver fibrogenic genes, GLI1 downstream genes were examined using western blot and real-time PCR analyses. GLI1 acetylation and LAP2 $\alpha$ -HDAC1 interaction were analyzed by coimmunoprecipitation. **Key Results:** In animal models, PB administration attenuated hepatic histopathological injury, collagen accumulation, and reduced the expression of fibrogenic genes. PB dose-dependently suppressed fibrotic marker expression in LX-2 cells and mouse pHSCs. Mechanistic studies showed PB inhibited GLI activity in a non-canonical Hedgehog signaling. PB blocked lamina-associated polypeptide 2  $\alpha$  (LAP2 $\alpha$ )/ histone deacetylase 1 (HDAC1) complex formation thereby inhibited HDAC1 mediated GLI1 deacetylation. PB downregulated the acetylation and expression of GLI1, and subsequently inhibiting HSC activation. **Conclusions and Implications:** PB exerted potent antifibrotic effects in vitro and in vivo by disrupting the LAP2 $\alpha$ /HDAC1 complex, increasing GLI1 acetylation and inactivating GLI1. This indicates that PB may be a potential therapeutic candidate for the treatment of liver fibrosis.

**Physalin B attenuates liver fibrosis via suppressing LAP2  $\alpha$ -HDAC1 mediated deacetylation of GLI1 and hepatic stellate cell activation**

**Running Title:** Physalin B attenuates liver fibrosis via suppressing deacetylation of GLI1

Xiaoyun Zhu, Shengtao Ye, Jie Li, Meihui Zhang, Yanqiu Zhang, Yingrong Leng, Ting Yang, Jianguang Luo, Xinlin Chen, Hao Zhang\*, Lingyi Kong\*

State Key Laboratory of Natural Medicines and Jiangsu Key Laboratory of Bioactive Natural Product Research, School of Traditional Chinese Pharmacy, China Pharmaceutical University, Nanjing 210009, China

\* Correspondence to:

Hao Zhang, State Key Laboratory of Natural Medicines and Jiangsu Key Laboratory of Bioactive Natural Product Research, School of Traditional Chinese Pharmacy, China Pharmaceutical University, 24 Tong Jia Xiang, Nanjing 210009, China. E-mail: [zhanghao@cpu.edu.cn](mailto:zhanghao@cpu.edu.cn) ;

Lingyi Kong, State Key Laboratory of Natural Medicines and Jiangsu Key Laboratory of Bioactive Natural Product Research, School of Traditional Chinese Pharmacy, China Pharmaceutical University, 24 Tong Jia Xiang, Nanjing 210009, China. E-mail: [cpu\\_lykong@126.com](mailto:cpu_lykong@126.com);

**Data availability:** The data that support the findings of this study are available from the corresponding author upon reasonable request.

**Funding:** This work was supported by National Natural Science Foundation of China (No. 82074068, 81872889) and Natural Science Foundation of Jiangsu Province (BK20181332) to Hao Zhang. The Drug Innovation Major Project (2018ZX09711-001-007 and 2018ZX09735002-003), the “Double First-Class” University Project (CPU2018GF03) to Lingyi Kong.

**Author contributions:** HZ and XYZ conceived the study and participated in the overall design, supervision, and coordination of the study. XYZ designed and performed most experiments. STY, JL, MHZ participated in molecular and cellular biological experiments. YRL, TY, YQZ participated in animal studies. HZ and XYZ wrote the manuscript. LYK supervised the overall project. All authors read and approved the manuscript.

**Acknowledgments:** We cordially wish to acknowledge the cellular platform and the pathology center for the excellent technical support.

**Conflicts of interest:** The authors declare no conflicts of interest.

**Ethics approval:** All mice received human care and animal experiments were approved by the University Committee on Use and Care of Animals of the China Pharmaceutical University (Nanjing, China). (Approval NO.2020-0701)

### Declaration of transparency and scientific rigour

This declaration acknowledges that this paper adheres to the principles for transparent reporting and scientific rigour of preclinical research as stated in the *BJP* guidelines for Design & Analysis, Immunoblotting and Immunohistochemistry, and Animal Experimentation, and as recommended by funding agencies, publishers and other organisations engaged with supporting research.

**Keywords:** Physalin B; Liver fibrosis; GLI1; Acetylation; LAP2 $\alpha$ ; HDAC1.

**Abbreviations:** PB, Physalin B; GLI1, glioma-associated oncogene homologue 1; LAP2 $\alpha$ , lamina-associated polypeptide 2  $\alpha$ ; HDAC1, histone hyperacetylation by histone deacetylase 1; HSCs, hepatic stellate cells; COL1A1, collagen type I  $\alpha$  1 chain; CCl<sub>4</sub>, carbon tetrachloride; BDL, bile duct ligation;  $\alpha$ -SMA,  $\alpha$ -smooth muscle actin; Coll1A1, collagen type I alpha 1;  $\alpha$ -SMA,  $\alpha$ -smooth muscle actin; TGF $\beta$ 1, transforming growth factor  $\beta$ 1; TIMP-1, TIMP metalloproteinase inhibitor 1; ALT, alanine aminotransferase; AST, aspartate aminotransferase; ECM, extracellular matrix.

### Bullet point summary:

*What is already known?*

GLI1 is a crucial factor in the pathogenesis of liver fibrosis.

LAP2 $\alpha$  forms an activating complex with HDAC1 to deacetylate/activate GLI1.

*What this study adds?*

The first observation that Physalin B attenuates liver fibrosis in two rodent models.

Physalin B blocks the interaction between LAP2 $\alpha$  and HDAC1 and promotes GLI1 acetylation.

*What is the clinical significance?*

PB may be a potential therapeutic candidate for liver fibrosis.

Blocking the interaction of LAP2 $\alpha$  and HDAC1 could be a new strategy for liver fibrosis therapy.

### Abstract

**Background and Purpose:** Liver fibrosis is one of the leading causes of morbidity and mortality worldwide of which no acceptable therapy exists. Accumulating evidence supports that glioma-associated oncogene homologue 1 (GLI1) is a potentially important therapeutic target for liver fibrosis. This study investigates the antifibrotic activities and potential mechanisms of Physalin B (PB), a natural Solanaceae compound.

**Experimental Approach:** Mice subjected to CCl<sub>4</sub> challenge and bile duct ligation were used to study the antifibrotic effects of PB *in vivo*. Mouse primary hepatic stellate cells (pHSCs) and human HSC line LX-2 also served as an *in vitro* liver fibrosis model. Liver fibrogenic genes, GLI1 downstream genes were examined using western blot and real-time PCR analyses. GLI1 acetylation and LAP2 $\alpha$ -HDAC1 interaction were analyzed by coimmunoprecipitation.

**Key Results:** In animal models, PB administration attenuated hepatic histopathological injury, collagen accumulation, and reduced the expression of fibrogenic genes. PB dose-dependently suppressed fibrotic marker expression in LX-2 cells and mouse pHSCs. Mechanistic studies showed PB inhibited GLI activity in a non-canonical Hedgehog signaling. PB blocked lamina-associated polypeptide 2  $\alpha$  (LAP2 $\alpha$ )/ histone deacetylase 1 (HDAC1) complex formation thereby inhibited HDAC1-mediated GLI1 deacetylation. PB downregulated the acetylation and expression of GLI1, and subsequently inhibiting HSC activation.

**Conclusions and Implications:** PB exerted potent antifibrotic effects *in vitro* and *in vivo* by disrupting the LAP2 $\alpha$ /HDAC1 complex, increasing GLI1 acetylation and inactivating GLI1. This indicates that PB may be a potential therapeutic candidate for the treatment of liver fibrosis.

## Introduction

Liver fibrosis, a wound-healing response to chronic liver injury, is characterized by excessive deposition of extracellular matrix (ECM) in the liver. During chronic liver damage, HSCs are continuously activated and converted into myofibroblasts, which are the major source of ECM and the principal cell type in liver fibrogenesis (Friedman, 2008). This transient response must be tightly controlled, otherwise, it would become persistent and lead to excessive matrix accumulation and fibrosis (Lee, Wallace & Friedman, 2015). Thus, potential therapies for these pathologies should ideally possess pro regenerative and antifibrotic properties, for example, the ability of controlling hepatocyte proliferation and inactivating activated HSC (Hernandez-Gea & Friedman, 2011). Currently, there are no approved drugs that can effectively reverse liver fibrosis, further highlighting the urgent clinical need for novel antifibrotic therapies.

GLI (glioma-associated oncogene homologue) was identified as a gene that is amplified in gliomas (McMillin et al., 2014), and it is one of the strongest transcriptional activators of Hh signaling pathway, can also be regulated independent of the canonical Hh signaling pathway. The TGF $\beta$  signaling pathway activates GLI1 even in the presence of SMO antagonist (Denkler et al., 2007). In injured organs, resident GLI1<sup>+</sup> cells were committed to the myofibroblast lineage, which directly regulates HSC fate (Machado & Diehl, 2018). Genetic ablation of GLI1<sup>+</sup> cells ameliorated fibrosis and improved organ function, providing a proof of principle for therapeutic targeting of GLI1<sup>+</sup> cells in fibrotic disease (Kramann et al., 2015). The aforementioned reports emphasize the importance of the mechanisms that terminate GLI1 activity and that may be impaired in disease. Hence, GLI1 is a potential biomarker and therapeutic target aiming at controlling activation of HSCs during liver fibrogenesis.

GLI1 acetylation, a modification that limits the activity of this transcription factor (Miele et al., 2017). Acetylation represents a key transcriptional event, finely tuned by histone acetyltransferases (HATs) and histone deacetylases (HDACs). It has been observed that loss of class I HDAC disrupts the transcriptional response to Hh activation, HDAC1 is shown to deacetylate the transcription factor GLI1 (Canettieri, Di Marcotullio, Coni, Greco & Gulino, 2010), which allows GLI1 to associate with chromatin and initiate transcription (Canettieri et al., 2010; Coni et al., 2013). Such deacetylation mechanisms are involved in GLI1-dependent cell proliferation, migration, differentiation, and survival.

Currently, few antifibrotic treatment strategies are available. Thus, there is an urgent clinical need for the development of antifibrotic candidates specifically targeting HSCs. Our study is engaged in evaluating

the antifibrotic activities of natural compounds. We have utilized a high-throughput drug screening model based on the COL1A1 promoter to filtrate potential anti-hepatic fibrosis agents from natural substances. Physalin B (PB), a natural component derived from one of the best-known traditional Chinese medicinal plants, *Physalis* species, Solanaceae, was speculated having potential therapeutic effect for liver fibrosis by us. Previous studies have described the biological functions of PB, including anti-inflammatory (Hsu et al., 2012; Yang, Yi, Wang, Xie, Sha & Dong, 2018), antimalarial (Magalhaes et al., 2006), proapoptotic (Soares et al., 2006), antinociceptive (Vandenbergh et al., 2008), and antitumor activities (Hsu et al., 2012; Ma, Han, Li, Hu & Zhou, 2015), but the effects of PB on liver fibrosis have not been reported thus far. We investigated the anti-fibrotic effects of PB on human stellate cell line LX-2, primary HSCs, and experimental hepatic fibrosis mice induced by CCl<sub>4</sub> and bile duct ligation (BDL), finally elucidated the potential mechanisms underlying its function *in vitro* and *in vivo*.

## 2 Methods

### 2.1 Animals and experimental design

All mice received human care and animal experiments were approved by the University Committee on Use and Care of Animals of the China Pharmaceutical University (Nanjing, China), (Resolution number, 202007001). Animal studies are reported in compliance with the ARRIVE guidelines (Lilley et al., 2020) and with the recommendations made by the British Journal of Pharmacology. Male C57BL/6J used for this study (18–20 g, specific -pathogen-free class) were purchased from Charles River Laboratories Co., Ltd (Beijing, China). Five-week-old mice were used for establishing CCl<sub>4</sub> and BDL-induced hepatic fibrosis model and 6–8-week-old mice were used for isolating mouse primary HSCs. Animals were maintained in an environmentally controlled room (pathogen-free, 20–24°C, 40–60% relative humidity and 12-hr alternating light/dark cycle). Laboratory animals were randomly assigned to groups of equal size. Analysis of all animal samples was carried out in a blinded manner.

### 2.2 Mouse model of CCl<sub>4</sub>-induced hepatic fibrosis

Forty mice were also assigned into five groups (control, CCl<sub>4</sub>-corn oil, and CCl<sub>4</sub>-PB groups) followed by a randomization procedure (<http://www.randomizer.org/>, Research Randomizer, RRID:SCR\_008563), with eight animals per group. A mouse model of liver fibrosis was established by intraperitoneally injecting of 10% CCl<sub>4</sub> mixed with oil for 4 weeks (0.25mL/kg body weight, thrice a week). Thirty-two mice were randomly divided into four groups (n = 8 mice per group): the model group (received only the CCl<sub>4</sub>-corn oil injection) and the PB-treated group (received the CCl<sub>4</sub> injection and a concurrent 1, 2.5, 5mg\*kg<sup>-1</sup> PB intraperitoneal injection every other day began during the CCl<sub>4</sub> treatment). The control group (n = 8) was intraperitoneally injected with corn oil alone for 8 weeks. The vehicle group (n = 8) was intraperitoneal injection with 2% DMSO as the. Blood samples (200 µl) were collected from the retro-orbital venous plexus of overnight-fasted mice and then the mice were killed under anaesthesia. Mouse liver maximum lobule was collected. Some liver tissue samples were fixed with 4% paraformaldehyde for subsequent histological examination and others were stored at -80°C until further experiments.

### 2.3 Bile duct ligation (BDL) surgery in mice

Forty mice were randomly assigned into five groups (sham, BDL-NS, and BDL-PB groups) followed by a randomization procedure (<http://www.randomizer.org/>, Research Randomizer, RRID: SCR\_008563), with eight animals per group. Thirty-two mice were prepared for BDL surgery. After the mice were anaesthetized with isoflurane, the mice abdomen was opened. The choledochal duct was isolated and ligated using surgical sutures. Twenty-four hours after surgery, animals subjected to BDL were randomly divided into three groups and received intraperitoneal injection daily with 1, 2.5, 5mg/kg PB solution (BDL-PB group) for 14 days. A sham operation was also performed on eight mice (sham group) to create a healthy control group. A normal 2%DMSO solution (2%DMSO group) was intraperitoneal injection daily on eight mice to create a vehicle group. After an overnight fast, blood samples were collected from the abdominal aorta and the animals were killed using isoflurane. Mice liver maximum lobule was collected. Some liver tissue samples were fixed with 4% paraformaldehyde for subsequent histological examination and others were stored at -80degC for

subsequent analyses.

## 2.4 Serum biochemical parameters

Serum levels of alanine aminotransferase (ALT) and aspartate aminotransferase (AST) were measured using standard enzymatic procedures according to the manufactures' instruction (Nanjing Jiancheng Bioengineering Institute, Nanjing, China).

## 2.5 Histological analysis of liver tissue samples

Formalin-fixed, paraffin-embedded liver tissue sections were stained with haematoxylin, eosin and sirius red. Liver necrosis, bile duct proliferation and hepatic inflammation were quantified in a blinded manner on a 1- to 5-point scale using a Leica DM1000 microscope. Sirius red- stained sections from each animal were observed at low magnification and analysed using ImageJ software to calculate the percentage of hepatic fibrous area.

## 2.6 Cell culture, isolation and treatment

LX-2 cells were received as a generous gift from Scott Friedman (Mount Sinai School of Medicine, New York). Cell lines were routinely tested for mycoplasma. LX-2 cells supplemented with 10% FBS and 1% penicillin/streptomycin (Invitrogen, Carlsbad, CA, USA). Upon reaching 60–80% confluences, the cells were starved in serum-free DMEM for 24 hr prior to treatment with 2 ng\*ml<sup>-1</sup> TGFβ1 and/or PB (dissolved in DMSO). Primary murine HSCs were isolated from the livers of male C57BL/6J mice aged 6-10 weeks according to a reported protocol that includes the following steps: in situ pronase/collagenase perfusion of mouse liver, perfused livers were minced, filtered through 70 μM cell strainer (BD Bioscience), and centrifuged at 50 g for 3 min to separate hepatocytes. HSCs were isolated according to the previously published method (Mederacke, Dapito, Affo, Uchinami & Schwabe, 2015), the supernatant was further centrifuged at 500 g for 10 min, resuspended in density gradient-based Nycodenz, and centrifuged at 1400 g for 17 min. HSCs were collected from the interface. Cells were cultured in DMEM (high glucose) containing 10% FBS and 1% antibiotics. Mouse pHSCs were plated in untreated flasks and can exhibit a fibroblast-like morphology after 7 days. Therefore, they did not need FBS-free starvation or TGFβ1 stimulation. HEK293T cells (RRID: CVCL\_0063) were cultivated in DMEM with 10% FBS and 1% antibiotics. All these cells were incubated at 37°C in a 5% CO<sub>2</sub> atmosphere. LX-2 and HEK293T cells were transiently transfected with plasmids or siRNAs using the Lipofectamine 3000 reagent (Invitrogen, 11668019) and Opti-MEM serum-free medium (Invitrogen, 1930104) according to the manufacturer's instructions.

## 2.7 Luciferase Reporter Assay

The pGL4.17-COL1A1 luciferase reporter plasmid is gift from Hongwei He (Peking Union Medical College, Beijing) (Zhao, Wang, Wang, Shao & He, 2015). LX-2 cells were transfected with pGL4.17-COL1A1 and pGMGLI-Lu luciferase reporter plasmid (Yesen, 11524ES03) then treated with PB (0.25, 0.5 and 1 μM) for 24 h. Cells were lysed and subjected to luciferase reporter assay by using DualLuciferase® Reporter Assay System (Vazyme, #DL101-01).

## 2.8 Quantitative real-time PCR

Total RNA was extracted from the liver tissues of the mice or LX-2 cells using Tripure reagent (Roche Diagnostics, Indianapolis, IN) as described by the manufacturer. cDNA synthesis was carried out with HiScript(r) II Q Select RT SuperMix for qPCR (Vazyme). Quantitative PCR was performed in biological triplicates using SYBR Green reagent (Vazyme). The level of GAPDH (human) or β-actin (mouse) RNA expression was used to normalize the data. PCR primer sequences are listed in Supplementary Table 1. A melting curve of each amplicon was determined to verify its specificity.

## 2.9 Immunoprecipitation and western blot analysis

RIPA lysate buffer (Beyotime Biotechnology, P0013B) containing 1% PMSF was used to extract the total proteins from cells and hepatic tissues. Protein concentrations were measured using a BCA kit (Beyotime

Biotechnology, P0009). After immunoprecipitating, proteins with the appropriate antibodies overnight at 4°C and incubating the complexes with Protein A/G Plus-agarose (Santa Cruz Biotechnology, sc-2003) for 4 hr at 4degC, total cell lysates were washed five times, mixed with 2x SDS loading buffer, and boiled for 10 min. Equal amounts of immunocomplexes or lysates were electrophoresed on SDS-PAGE gels and transferred to PVDF membranes. Membranes were blocked with 5% skim milk in PBS-T buffer (PBS containing 0.2% Tween 20) at room temperature for 1 hr and then immunoblotted with primary antibodies overnight at 4degC. Peroxidase-conjugated secondary antibodies were then applied to the membranes and incubated for 1 hr at room temperature. Electrochemiluminescence was performed according to the manufacturer's instructions with a BIO-RED ChemiDoc XRS+ imaging system.  $\beta$ -actin was served as an internal control. Both immunoprecipitation assay and western blot have been conducted the experimental detail provided conforms with BJP Guidelines (Alexander et al., 2018). The immuno-related procedures used comply with the recommendations made by the British Journal of Pharmacology.

## 2.10 Nuclear and cytoplasmic protein extraction

Nuclear and cytoplasmic proteins were extracted from LX-2 cells using the Nuclear-Cytosol Extraction Kit (Beyotime Biotechnology, P0028). The extracts were mixed with 2× SDS loading buffer and analysed using western blot as described above.

## 2.11 Confocal assay

LX-2 cells were plated on glass cover slips in a dish. After exposure to different treatments, the cells were washed three times with PBS, fixed with 4% paraformaldehyde for 20 min and then permeabilized with 0.5% Triton X-100 for 30 min at room temperature. Next, the cells were incubated with specific primary antibodies overnight at 4degC. Cells were washed three times with PBS and subsequently incubated with a fluorochrome-labelled secondary antibody for 1 hr at room temperature. The cells were then rinsed three times with PBS and the nuclei were counterstained with DAPI for 5 min at room temperature. Images were captured using a Leica SP2 confocal microscope (Leica Microsystems, Exton, PA)

## 2.12 Reagents

Physalin B (purity [?]98%) were separated and purified in our laboratory; their structures, shown in Figure 1A, were confirmed by comparing the IR, 1H and 13C nuclear magnetic resonance and MS data with reported data (Zheng, Chen, Liu, Liang & Hong, 2016). Calyx Seu Fructus Physalis (3 kg) were extracted with 95% ethanol for three times. After solvent removal, the crude extractive was separated successively with ethanol (40%, 80%, 100%) on macroporous resin and obtained fraction B. The Fr.B was partitioned with H<sub>2</sub>O, ethyl acetate, methylene chloride and petroleum ether. Fractionation of the methylene chloride extract using silica gel column, eluting with CH<sub>2</sub>Cl<sub>2</sub>: CH<sub>3</sub>OH (100: 1-5: 1) to obtain subfraction B. Subfraction B were chromatographed over a MCI, eluting with gradient mixtures of CH<sub>3</sub>OH-H<sub>2</sub>O (from 30: 70 to 100: 0). Finally, compound PB was obtained by ODS and P-HPLC. Its structure was identified by comparing 1H, 13C -NMR data with those of literature (Zheng, Luan, Chen, Ren & Wu, 2012). The compound was more than 98% pure and dissolved in DMSO at a stock concentration of 5 mM.

An anti- $\alpha$ -smooth muscle actin antibody ( $\alpha$ -SMA; ab7817), anti-COL1A1 (ab34710) and anti-LAP2 $\alpha$  (ab5162) antibodies were purchased from Abcam. Anti-GLI1 (#2553), anti-Acetylated-Lysine (#9441), anti-Flag-Tag (#14793) and anti-Myc-Tag (#2276) antibodies and normal rabbit IgG (#2729) were obtained from Cell Signaling Technology (Danvers, MA, USA). Anti-HA-Tag (51064-2-AP and 66006- 1-Ig), anti-HDAC1 (66085-1-Ig) antibodies were purchased from Proteintech (Wuhan, China). Vorinostat (HY-10221), TGF $\beta$ 1 (HY-P7118), GANT61(HY-13901) was acquired from MCE (Shanghai, China). GLI1 siRNA, LAP2 $\alpha$  siRNA were acquired from RiboBio (Guangzhou, China). was obtained from MCE (Shanghai, China). Additional materials were obtained from commercial sources.

## 2.13 Statistical analysis.

The results are presented as mean  $\pm$  SEM. Statistical differences between two groups were analyzed by the unpaired Student's t test with a two-tailed distribution. Differences between multiple groups of data were

analyzed by one-way ANOVA with Bonferroni correction (Graph Pad Prism 8.0, San Diego, CA, USA). P-values less than 0.05 were considered statistically significant. Statistical analysis was undertaken only for at least five independent experiments and other data was not statistically analysed owing to group sizes of  $n < 5$ . The data were analysed using one-way ANOVA with Tukey's post hoc test when F achieved  $P < 0.05$  and there was no significant variance in homogeneity. The results were considered statistical significance at  $P < 0.05$ . The data and statistical analysis comply with the recommendations of the British Journal of Pharmacology on experimental design and analysis in pharmacology (Curtis et al., 2018).

## 2.14 Nomenclature of targets and ligands

Key protein targets and ligands in this article are hyperlinked to corresponding entries in <http://www.guidetopharmacology.org>, the common portal for data from the IUPHAR/BPS Guide to PHARMACOLOGY (Harding et al., 2018), and are permanently archived in the Concise Guide to PHARMACOLOGY 2019/20 (Alexander et al., 2019).

## 3 Results

### 3.1 PB inhibited the proliferation and activation of HSCs

HSC proliferation and transformation play vital roles in the process of fibrosis (Tan, Liu, Ke, Jiang & Wu, 2020; Wu et al., 2016). Thus, intervention of HSC proliferation, apoptosis and inhibition of the fibrogenic function, are proposed therapeutic approaches to reverse liver fibrosis. To evaluate the anti-hepatic fibrosis effect of drug candidates, we employed a luciferase screening cell model based on the COL1A1 promoter activity. Results of dual-luciferase reporter assay showed that COL1A1 promoter activity was significantly increased with TGF $\beta$ 1 treatment in LX-2 cells. PB significantly inhibited COL1A1 promoter luciferase activity in a concentration-dependent manner (Figure 1B). To determine whether PB has an effect on LX-2 cell proliferation and apoptosis, LX-2 cells were treated with 0.25 $\mu$ M, 0.5 $\mu$ M or 1 $\mu$ M PB, and the cell proliferation and apoptosis were measured by CCK-8 assay and Annexin V-propidium iodide (PI) staining, respectively. The results showed that PB could inhibit TGF $\beta$ 1 induced HSC proliferation, however, scarcely influenced the apoptosis of LX-2 cells (Figure 1C and Supplementary Fig. 1A). These results indicated that PB is a potential anti-liver fibrosis drug.

Next, we assessed the effect of PB on HSC activation. In the context of FBS-free starvation and TGF $\beta$ 1 stimulation, LX-2 cells display an activated phenotype *in vitro*. PB inhibited the mRNA expression of various fibrogenic genes, including *TGF $\beta$ 1*,  *$\alpha$ -SMA*, and *COL1A1* in LX-2 cells (Figure 1D). The protein expression also showed a corresponding decrease after treatment with PB in LX-2 cells (Figure 1E). Meanwhile, the expression of  $\alpha$ -SMA was assessed by immunofluorescence, which showed that  $\alpha$ -SMA expression was increased by the TGF $\beta$ 1 treatment while significantly attenuated by PB in LX-2 cells (Figure 1F). We then confirmed the effect of PB on cultured mouse pHSC. As mouse pHSCs exhibit self-activation, they do not require starvation and stimulation during *in vitro* culture. Similarly, RT-qPCR and western blot results showed that PB reduced the mRNA and protein expression of  $\alpha$ -SMA, immunofluorescence analysis further confirmed that PB could decrease  $\alpha$ -SMA expression during differentiation (Figure 1G-I). These results suggest that PB is a potent antifibrogenic agent in HSC activation.

### 3.2 PB ameliorated CCl<sub>4</sub>-induced liver injury and hepatic fibrosis in mice

In order to evaluate whether large doses of PB has any hepatotoxicity, mice were intraperitoneal injection of PB 40mg/kg. HE staining, Sirius red staining and Masson staining showed that PB (40mg/kg) did not cause any pathological or fibrous damage (Supplementary Fig. 1B). Mice were intraperitoneal injection with 2% DMSO as the vehicle group. Similarly, HE staining, Sirius red staining and Masson staining showed that 2% DMSO did not cause any pathological or fibrous damage (Supplementary Fig. 1C). Based on these results, we next evaluated the anti-hepatic fibrosis effect of PB in mouse fibrosis models *in vivo*.

Carbon tetrachloride (CCl<sub>4</sub>) is a hepatotoxin that has been used extensively to induce liver injury. It induces liver fibrosis by producing various reactive metabolites and damaging hepatocytes. To assess the pharmaceutical activities of PB *in vivo*, we performed CCl<sub>4</sub> challenge in mice. After 4 weeks of CCl<sub>4</sub> injections,

the mice exhibited marked increases in hepatic inflammatory cell infiltration, mild thickening of the central venous wall and fibrous hyperplasia. However, PB treatment ameliorated these pathological changes and protected against CCl<sub>4</sub>-induced fibrosis (Figure 2A). Serum ALT and AST levels were significantly elevated in the CCl<sub>4</sub>-treated mice, while decreased in PB treated group indicating improved liver injury (Figure 2B). The severity of liver fibrosis was also biochemically assessed by measuring the hepatic hydroxyproline content. PB markedly decreased the CCl<sub>4</sub>-induced increase of hydroxyproline content (Figure 2C). Sirius red and Masson's trichrome staining visualizes collagen, which is used to evaluate the degree and characteristics of fibrosis. Sirius Red, Masson's trichrome stained liver sections indicated that fibrous collagen deposition, fibroplasia, and bridging fibrosis significantly decreased in PB treated mice (Figure 2D). The expression of hepatic fibrogenic markers, including  $\alpha\text{SMA}$ , *Col1a1*, *Tgfb1* and tissue inhibitor of metalloproteinase 1 (*Timp1*) were detected to assess the antifibrotic effects of PB *in vivo*. PB treatment significantly decreased the mRNA expression of these fibrogenic genes. Western blot assays also validated that PB treatment decreased  $\alpha\text{-SMA}$  and COL1A1 expression in the liver tissues (Figure 2E, F). Accordingly, PB has the potential to inhibit the progression of CCl<sub>4</sub>-induced hepatic fibrosis in mice.

### 3.3 PB ameliorated BDL-induced liver injury and reduced hepatic fibrosis indexes

Biliary duct ligation (BDL) in mice can cause severe hepatocyte injury and liver fibrosis, and this model has also been widely used to analyze the molecular mechanism of liver injury. H&E staining assays demonstrated that the liver histological structure of the BDL group was severely damaged. Extensive liver parenchyma necrosis and newly formed bile ducts were observed in BDL model group. As expected, these pathological changes were ameliorated by PB treatment (Figure 3A). The serum ALT, AST levels were significantly increased in the BDL mice compared with those of the sham mice, and statistical reductions in these values was observed when the BDL mice were treated with PB (Figure 3B). PB dramatically decreased liver hydroxyproline concentration caused by BDL (Figure 3C). In the BDL group, Sirius red and Masson's trichrome stained collagen fibrils extended not only to the portal areas but also to the hepatic parenchyma. PB supplementation strongly attenuated liver collagen deposition, as shown by the substantial decrease in positively stained areas (Figure 3D). The mRNA and/or protein levels of fibrogenic markers were prominently increased in the BDL treated group compared with the control group, while they were dramatically lowered by the PB intervention (Figure 3E, F). These data indicate that PB can ameliorate the BDL-induced liver injury and may play a therapeutic role in hepatic fibrosis.

### 3.4 PB inhibited liver fibrosis through downregulation of GLI1 expression

Recent studies have reported that a positive correlation exists between HSC activation and GLI1 overexpression (Chung et al., 2016; Guerrero-Juarez & Plikus, 2017; Zhang et al., 2017). Growing evidence indicate that GLI1 is a critical regulator of adult liver repair and hence, a potential diagnostic and/or therapeutic target in cirrhosis (Chen et al., 2020; Seki, 2016; Zhang et al., 2017). Based on the above, we investigated whether GLI1 was involved in the anti-hepatic fibrosis activity of PB. To determine whether PB regulated GLI1 activity, GLI-dependent luciferase activity was monitored, and the results showed that PB strongly repressed GLI-luciferase activities (Figure 4A). In addition, TGF $\beta$ 1 stimulation significantly increased GLI1 expression, while PB treatment decreased GLI1 expression (Figure 4B, C). Similar results were also observed in PB treated mouse pHSCs (Figure 4D, E). However, RT-qPCR results showed that PB scarcely influenced the GLI2, GLI3 expression in LX-2 cells (Supplementary Fig. 2A). Furthermore, PB treatment downregulated GLI1 protein expression in BDL-induced fibrotic liver tissues (Figure 4F).

Next, we wonder whether PB mediated anti-fibrosis effect dependent on GLI1. First, we verified that knockdown of *GLI1* suppressed the mRNA and protein expression of fibrogenic in LX-2 cells (Figure 5A, B). These results indicate that GLI1 indeed plays an important role in HSCs activation. Next, we measured Collagen I and  $\alpha\text{SMA}$  expression in PB treated LX-2 cells with or without *GLI1* knockdown. As shown in Fig 5C, PB could not further reduce the Collagen I and  $\alpha\text{SMA}$  expression in the context of GLI deficiency. In addition, the similar results were achieved when the cells were treated with GANT61, the most-widely used specific inhibitor of GLI1. GANT61 treatment decreased GLI-luciferase activity and GLI1 mRNA levels (Supplementary fig. 2B, C). However, the combination of PB and GANT61 showed no additive effect on the

reduction of fibrogenic gene expression in LX-2 cells (Supplementary Fig. 2D). Furthermore, overexpression of GLI1 promoted Collagen I and  $\alpha$ SMA expression, and reversed PB mediated inhibition of aforementioned proteins (Figure 5D). These results illustrated that PB inhibited HSC activation via downregulation of GLI1 expression.

### 3.5 PB blocked the nuclear localization of GLI1 in HSCs

Previous findings had shed light on GLI1 activity, which is tightly controlled through the regulation of nuclear import and the modulation of protein stability (Gulino, Di Marcotullio, Canettieri, De Smaele & Screpanti, 2012). GLI1 nucleus localization is critical for its growth-promoting function. Recently, Zhang et al. reported that GLI1 nuclear translocation leads to HSC contraction and cirrhotic portal hypertension (Zhang et al., 2020). We next tested if PB influenced the GLI1 nuclear localization. Expectedly, PB treatment blocked the translocation of GLI1 from the cytoplasm to the nucleus in a dose-dependent manner (Figure 6A). Nuclear and cytoplasmic fractionation analysis for GLI1 distribution reciprocated the immunofluorescence experiments in both LX-2 cells and mouse pHSCs (Figure 6B, C). Given that nuclear translocation of GLI1 resulting in increased GLI1 target gene expression (Kim, Kim, Cho, Kim, Kim & Cheong, 2010), we then measured GLI1 downstream target genes. The mRNA expression of well-known GLI1 downstream genes, including *HHIP*, *CYCLIN D*, *CYCLIN E* and *C-MYC* were dramatically down-regulated in both PB-treated LX-2 cells and BDL-PB treated mouse liver samples (Figure 6D, E). Similarly, GLI1 downstream genes were reduced in GANT61 treated LX-2 cells, whereas the combination of PB and GANT61 showed no additive effect on the reduction of downstream genes expression in LX-2 cells (Supplementary Fig. 2E). Taken together, these results indicated that PB repress the translocation of GLI1 from the cytoplasm to the nucleus, decreasing the expression of the downstream target genes.

### 3.6 PB inhibited LAP2 $\alpha$ -HDAC1 mediated deacetylation of GLI1

Published literatures suggest that GLI1 is temporarily inactive by acetylation (AcGLI1), therefore acetylation is an important modification to regulate cellular GLI1 (Coni et al., 2017; Mirza et al., 2019). Thus, we speculated that PB may affect the acetylation of GLI1 to regulate its activity. Indeed, anti-acetylated lysine immunoprecipitates indicated that GLI1 are constitutively acetylated with PB treatment (Figure 7A). Acetylation directly inhibits the expression of transcription factors (Gurung, Feng & Hua, 2013), thus PB may inhibit liver fibrosis by upregulating the acetylation of GLI1, which inactivates it.

It has been reported that the acetylation of GLI1 is regulated by HDAC1 (Canettieri et al., 2010; Falkenberg et al., 2016) and LAP2 $\alpha$  (Mirza et al., 2019). Mechanistically, LAP2 $\alpha$  recruits HDAC1 to GLI1, physically interacts with HDAC1, and scaffolds a complex with GLI1 (Mirza et al., 2019). Next, we wonder whether PB showed any effect on LAP2 $\alpha$  and HDAC1 expression. However, no significant protein variations were observed in both LAP2 $\alpha$  and HDAC1 after PB treatment in LX-2 cells (Figure 7B). Given that LAP2 $\alpha$ /HDAC1 mediated GLI1 deacetylation play an important role in GLI1 activity, we next wonder whether PB affect LAP2 $\alpha$ /GLI1 interaction or LAP2 $\alpha$ /HDAC1 complex formation. As shown in Fig 7C, PB showed no effect on the interaction between LAP2 $\alpha$ /GLI1, however, strongly inhibited the LAP2 $\alpha$ /HDAC1 complex formation in HEK 293T cells (Figure 7D). Congruently, endogenous LAP2 $\alpha$  and HDAC1 interaction was significantly disrupted by the PB treatment in LX-2 cells (Figure 7E), and this interaction was also reduced in CCl<sub>4</sub>-induced mouse fibrotic liver tissue treated with PB (Figure 7F).

Previous studies have demonstrated that nucleoplasmic complex LAP2 $\alpha$ -HDAC1 could protect GLI1 from acetylation and promote GLI1 activation (Mirza et al., 2019). As described in the above co-IP results, confocal microscopy assay was used to determine the subcellular localization of HDAC1 (red) and LAP2 $\alpha$  (green) to confirm this result *in situ*. Our results showed that PB had no influence on the nuclear localization of LAP2 $\alpha$  with or without TGF $\beta$ 1 treatment. However, PB obviously decrease the nuclear localization of HDAC1 after TGF $\beta$ 1 treatment (Figure 7G), indicating that PB administration may disturb the intracellular colocalization of LAP2 $\alpha$  with HDAC1. These results indicated that, instead of interfering with LAP2 $\alpha$  and GLI1 interaction, PB inhibited LAP2 $\alpha$ -HDAC1 complex formation, which may responsible for PB mediated GLI1 inactivation.

Next, we employed the histone deacetylase inhibitor vorinostat to further validate the results. Vorinostat decreased the levels of fibrogenic markers which is in consistent with previous published results (Park et al., 2014), and no further reduction was observed when combination with PB (Figure 8A). Immunofluorescence assay further confirmed that PB and vorinostat downregulated GLI1 expression and nuclear localization (Figure 8B). In addition, PB and vorinostat increased the acetylation of GLI1 (Figure 8C). Due to the protective effect of LAP2 $\alpha$  on GLI1 deacetylation, we next verify that whether LAP2 $\alpha$  deficiency can attenuate HSC activation by treating LX-2 cells with LAP2 $\alpha$  siRNA. The fibrogenic markers were suppressed in LAP2 $\alpha$  siRNA treated LX-2 cells (Figure 8D, E). Similarly, combination of LAP2 $\alpha$  silencing and PB treatment blocked nucleus translocation of GLI1 in LX-2 cells (Figure 8F). In addition, LAP2 $\alpha$ -silencing and PB treatment increased GLI1 acetylation (Figure 8G). Taken together, our results indicate that PB interferes with LAP2 $\alpha$ -HDAC1 complex formation, thereafter inhibits GLI1 deacetylation and downstream signaling. PB could be a promising therapeutic agent for liver fibrosis.

#### 4. Discussion

Fibrosis is a complex disease, driven at the cellular level by activation of quiescent HSCs and characterized by the sustained induction of a fibrotic gene program (Ding et al., 2015). The importance of preventing HSC activation during liver fibrosis treatment is undisputed. Traditional Chinese medicine which is composed of variant monomeric compounds from herbs are potential therapeutics for liver fibrosis. The natural product PB isolated from a Chinese herb *Physalis* species, Solanaceae, exhibited promising suppressive effect on liver fibrosis in two classic animal models and HSCs. The mechanism of such effect may be associated with inhibiting of the LAP2 $\alpha$  and HDAC1 interaction and regulating GLI1 acetylation. This conclusion is based on four major observations: i) BDL and CCl<sub>4</sub>-challenged mice treated with PB exhibited histological amelioration of liver damage and fibrosis. ii) The mRNA and protein levels of liver fibrogenic markers were downregulated by PB administration *in vitro* and *in vivo*. iii) We identify the role of PB in repressing GLI1 independent of the canonical Hh signaling pathway. PB increased the acetylation of GLI1 and blocked nuclear translocation of GLI1. iv) PB inhibited the LAP2 $\alpha$ -HDAC1 complex formation, which increased acetylation of GLI1 and exerted a therapeutic effect on hepatic fibrosis.

Increasing evidence showed that GLI1 is indispensable in liver pathophysiology. Recently literature reported that smoothened-independent GLI1 signaling directs differentiation of HPCs to fibrogenic cholangiocytes, and that it is upregulated during this fibrosis progression, while inhibiting the GLI1 expression suppresses fibrosis progression (Chen et al., 2020). GLI1 also plays an important role in activation of HSCs (Zhang et al., 2020), and GLI1 targeted inhibitors have been reported to improve fibrosis in mice and humans (Guerrero-Juarez & Plikus, 2017). GLI1 is regulated by different cascades, including the hedgehog and TGF pathways (Nye et al., 2014). After TGF $\beta$ 1 treatment, elevated expression of GLI1 and the nuclear localization of GLI1 in normal fibroblasts, keratinocytes, and various cell lines has been detected (Dennler et al., 2007; Katoh & Katoh, 2009), which was in accordance with our findings. In the present study, we found that PB inhibited expression of GLI1 and reduced the nuclear localization of GLI1, reversed the TGF $\beta$ 1-induced upregulation of myofibroblastic markers ( $\alpha$ -SMA and collagen I). On the contrary, overexpression of GLI1 increased the level of myofibroblastic markers in HSCs and reversed anti-fibrotic effect of PB. Based on these results, GLI1 can upregulate fibrogenic gene expression and promoted liver fibrosis, thus, blocking GLI1 is anticipated as a promising strategy. PB may inhibit liver fibrosis, as well as TGF $\beta$ 1 induced HSC activation through inhibiting GLI activity.

Acetylation is a posttranslational modification that can either alters the biological activities of proteins or alter subcellular localization (Blanco-Garcia, Asensio-Juan, de la Cruz & Martinez-Balbas, 2009; Nye et al., 2014). Previous investigates have shown that HDACs are a group of enzymes capable of removing acetyl groups from histone and other proteins (Kim et al., 2010), and that activity and recruitment are required for transcriptional activation of genes including *Gja1*, *Irf1*, and *Gli1* (Zupkovitz et al., 2006). Among HDACs, HDAC1 is positive modulators of the activator members of the GLI family (Canettieri et al., 2010). GLI1 physically interacts with HDAC1, and HDAC1-mediated deacetylation of GLI1 results in the transcriptionally active (Canettieri et al., 2010; Falkenberg et al., 2016; Geng et al., 2018; Gurung, Feng & Hua, 2013).

GLI1 deacetylation leads to the growth of medulloblastoma (Canettieri et al., 2010) and is increased in resistant basal cell carcinomas (Mirza et al., 2019). Conversely, in medulloblastoma and glioblastoma cells, the reduction of GLI1 deacetylation leads to decreased proliferation and increased apoptosis (Mazza et al., 2013). In accordance with these studies, we showed that PB increased GLI1 acetylation indicating an inactive state, and decreased the expression of  $\alpha$ SMA and COL1A1 in HSCs, thereafter preventing hepatic fibrosis. LAP2 $\alpha$  acts as a scaffold to recruit HDAC1 to GLI1 (Gotic & Foisner, 2010), GLI1 deacetylation increased GLI1 association with LAP2 $\alpha$  to form an activating complex that withstood stringent high-salt conditions (Mirza et al., 2019). Our study identified that PB had no effect on the total expression of HDAC1 and LAP2 $\alpha$ , but it prevented LAP2 $\alpha$  from recruiting HDAC1 and inhibited the formation of HDAC1-LAP2 $\alpha$  complex, thus downregulates the expression of GLI1 and its downstream target genes. Whereas, PB did not directly affect the interaction between LAP2 $\alpha$ -GLI1. In addition, it was reported that liver fibrosis can be blocked by induction of HDAC inhibitors (Liu et al., 2013). Loh et al. showed that potent and selective inhibitors of class I only HDAC enzymes profoundly inhibit hepatocyte death and type 2 inflammation to prevent TAA-induced liver fibrosis in mice (Loh et al., 2019). Previous studies have demonstrated that LAP2 $\alpha$  localizes in the nucleoplasm is highly influential on cell proliferation and differentiation in regenerated tissue (Vidak, Kubben, Dechat & Foisner, 2015). LAP2 $\alpha$  overexpression resulted in GLI1 hyperactivation, whereas knockdown depressed GLI1 expression in basal cell carcinomas cells (Mirza et al., 2019). In our system, we found that LAP2 $\alpha$  deficiency reduced the expression of myofibroblastic markers thereby attenuate HSC activation. Our investigation is the first revealing that PB inhibits liver fibrosis by impairing HDAC1-LAP2 $\alpha$ -GLI1 complex.

In summary, PB, a monomeric component of traditional Chinese medicine, is proved to ameliorate liver damage and fibrosis in BDL and CCl<sub>4</sub>-treated mice. We evaluated the antifibrotic effect of PB on both HSCs and liver tissues, and revealed that the underlying mechanism of PB involves HDAC1/LAP2 $\alpha$ -mediated GLI1 deacetylation. This study is the first showing that PB inhibited the formation of HDAC1-LAP2 $\alpha$  complex. Based upon these findings, PB exerts therapeutic effects on liver fibrosis, which qualifies it being a novel candidate for hepatic fibrosis treatment in the near future.

## References

- Alexander SPH, Kelly E, Mathie A, Peters JA, Veale EL, Armstrong JF, *et al.* (2019). THE CONCISE GUIDE TO PHARMACOLOGY 2019/20: Transporters. *Br J Pharmacol* 176 Suppl 1: S397-S493.
- Alexander SPH, Roberts RE, Broughton BRS, Sobey CG, George CH, Stanford SC, *et al.* (2018). Goals and practicalities of immunoblotting and immunohistochemistry: A guide for submission to the British Journal of Pharmacology. *Br J Pharmacol* 175: 407-411.
- Blanco-Garcia N, Asensio-Juan E, de la Cruz X, & Martinez-Balbas MA (2009). Autoacetylation regulates P/CAF nuclear localization. *J Biol Chem* 284: 1343-1352.
- Canettieri G, Di Marcotullio L, Coni S, Greco A, & Gulino A (2010). Turning off the switch in medulloblastoma: the inhibitory acetylation of an oncogene. *Cell Cycle* 9: 2047-2048.
- Canettieri G, Di Marcotullio L, Greco A, Coni S, Antonucci L, Infante P, *et al.* (2010). Histone deacetylase and Cullin3-REN(KCTD11) ubiquitin ligase interplay regulates Hedgehog signalling through Gli acetylation. *Nat Cell Biol* 12: 132-142.
- Chen J, Hu Y, Fang J, Chen L, Mu Y, Liu W, *et al.* (2020). GLI1, but not smoothened-dependent, signaling in hepatic progenitor cells promotes a ductular reaction, which aggravates liver fibrosis. *Journal of Hepatology* 73.
- Chung SI, Moon H, Ju HL, Cho KJ, Kim DY, Han KH, *et al.* (2016). Hepatic expression of Sonic Hedgehog induces liver fibrosis and promotes hepatocarcinogenesis in a transgenic mouse model. *J Hepatol* 64:618-627.
- Coni S, Antonucci L, D'Amico D, Di Magno L, Infante P, De Smaele E, *et al.* (2013). Gli2 Acetylation at Lysine 757 Regulates Hedgehog-Dependent Transcriptional Output by Preventing Its Promoter Occupancy.

Plos One 8.

Coni S, Mancuso AB, Di Magno L, Sdruscia G, Manni S, Serrao SM, *et al.* (2017). Selective targeting of HDAC1/2 elicits anticancer effects through Gli1 acetylation in preclinical models of SHH Medulloblastoma. *Sci Rep* 7: 44079.

Curtis MJ, Alexander S, Cirino G, Docherty JR, George CH, Giembycz MA, *et al.* (2018). Experimental design and analysis and their reporting II: updated and simplified guidance for authors and peer reviewers. *Brit J Pharmacol* 175: 987-993.

Dennler S, Andre J, Alexaki I, Li A, Magnaldo T, ten Dijke P, *et al.* (2007). Induction of sonic hedgehog mediators by transforming growth factor-beta: Smad3-dependent activation of Gli2 and Gli1 expression in vitro and in vivo. *Cancer Res* 67: 6981-6986.

Ding N, Hah N, Yu RT, Sherman MH, Benner C, Leblanc M, *et al.*(2015). BRD4 is a novel therapeutic target for liver fibrosis. *Proc Natl Acad Sci U S A* 112: 15713-15718.

Falkenberg KJ, Newbold A, Gould CM, Luu J, Trapani JA, Matthews GM, *et al.* (2016). A genome scale RNAi screen identifies GLI1 as a novel gene regulating vorinostat sensitivity. *Cell Death Differ* 23: 1209-1218.

Friedman SL (2008). Mechanisms of hepatic fibrogenesis. *Gastroenterology* 134: 1655-1669.

Geng Y, Liu J, Xie Y, Jiang H, Zuo K, Li T, *et al.* (2018). Trichostatin A promotes GLI1 degradation and P21 expression in multiple myeloma cells. *Cancer Manag Res* 10: 2905-2914.

Gotic I, & Foisner R (2010). Multiple novel functions of lamina associated polypeptide 2 alpha in striated muscle. *Nucleus-Phila* 1: 397-401.

Guerrero-Juarez CF, & Plikus MV (2017). Gli-fully Halting the Progression of Fibrosis. *Cell Stem Cell* 20: 735-736.

Gulino A, Di Marcotullio L, Canettieri G, De Smaele E, & Screpanti I (2012). Hedgehog/Gli control by ubiquitination/acetylation interplay. *Vitam Horm* 88: 211-227.

Gurung B, Feng Z, & Hua X (2013). Menin directly represses Gli1 expression independent of canonical Hedgehog signaling. *Mol Cancer Res* 11: 1215-1222.

Harding SD, Sharman JL, Faccenda E, Southan C, Pawson AJ, Ireland S, *et al.* (2018). The IUPHAR/BPS Guide to PHARMACOLOGY in 2018: updates and expansion to encompass the new guide to IMMUNOPHARMACOLOGY. *Nucleic Acids Res* 46: D1091-D1106.

Hernandez-Gea V, & Friedman SL (2011). Pathogenesis of Liver Fibrosis. *Annu Rev Pathol-Mech* 6: 425-456.

Hsu CC, Wu YC, Farh L, Du YC, Tseng WK, Wu CC, *et al.* (2012). Physalin B from *Physalis angulata* triggers the NOXA-related apoptosis pathway of human melanoma A375 cells. *Food Chem Toxicol* 50:619-624.

Katoh Y, & Katoh M (2009). Integrative genomic analyses on GLI1: positive regulation of GLI1 by Hedgehog-GLI, TGFbeta-Smads, and RTK-PI3K-AKT signals, and negative regulation of GLI1 by Notch-CSL-HES/HEY, and GPCR-Gs-PKA signals. *Int J Oncol* 35:187-192.

Kim JY, Shen S, Dietz K, He Y, Howell O, Reynolds R, *et al.*(2010). HDAC1 nuclear export induced by pathological conditions is essential for the onset of axonal damage. *Nat Neurosci* 13:180-U163.

Kim K, Kim KH, Cho HK, Kim HY, Kim HH, & Cheong J (2010). SHP (small heterodimer partner) suppresses the transcriptional activity and nuclear localization of Hedgehog signalling protein Gli1. *Biochem J* 427: 413-422.

- Kramann R, Schneider RK, DiRocco DP, Machado F, Fleig S, Bondzie PA, *et al.* (2015). Perivascular Gli1+ progenitors are key contributors to injury-induced organ fibrosis. *Cell Stem Cell* 16: 51-66.
- Lee YA, Wallace MC, & Friedman SL (2015). Pathobiology of liver fibrosis: a translational success story. *Gut* 64: 830-841.
- Lilley E, Stanford SC, Kendall DE, Alexander SPH, Cirino G, Docherty JR, *et al.* (2020). ARRIVE 2.0 and the British Journal of Pharmacology: Updated guidance for 2020. *Br J Pharmacol* 177:3611-3616.
- Liu YQ, Wang Z, Wang JN, Lam W, Kwong S, Li FR, *et al.* (2013). A histone deacetylase inhibitor, largazole, decreases liver fibrosis and angiogenesis by inhibiting transforming growth factor-beta and vascular endothelial growth factor signalling. *Liver International* 33:504-515.
- Loh Z, Fitzsimmons RL, Reid RC, Ramnath D, Clouston A, Gupta PK, *et al.* (2019). Inhibitors of class I histone deacetylases attenuate thioacetamide-induced liver fibrosis in mice by suppressing hepatic type 2 inflammation. *Br J Pharmacol* 176: 3775-3790.
- Ma YM, Han W, Li J, Hu LH, & Zhou YB (2015). Physalin B not only inhibits the ubiquitin-proteasome pathway but also induces incomplete autophagic response in human colon cancer cells in vitro. *Acta Pharmacol Sin* 36: 517-527.
- Machado MV, & Diehl AM (2018). Hedgehog signalling in liver pathophysiology. *J Hepatol* 68: 550-562.
- Magalhaes HI, Veras ML, Torres MR, Alves AP, Pessoa OD, Silveira ER, *et al.* (2006). In-vitro and in-vivo antitumour activity of physalins B and D from *Physalis angulata*. *J Pharm Pharmacol* 58:235-241.
- Mazza D, Infante P, Colicchia V, Greco A, Alfonsi R, Siler M, *et al.* (2013). PCAF ubiquitin ligase activity inhibits Hedgehog/Gli1 signaling in p53-dependent response to genotoxic stress. *Cell Death Differ* 20: 1688-1697.
- McMillin M, Galindo C, Pae HY, Frampton G, Di Patre PL, Quinn M, *et al.* (2014). Gli1 activation and protection against hepatic encephalopathy is suppressed by circulating transforming growth factor beta1 in mice. *J Hepatol* 61: 1260-1266.
- Mederacke I, Dapito DH, Affo S, Uchinami H, & Schwabe RF (2015). High-yield and high-purity isolation of hepatic stellate cells from normal and fibrotic mouse livers. *Nat Protoc* 10: 305-315.
- Miele E, Po A, Begalli F, Antonucci L, Mastronuzzi A, Marras CE, *et al.* (2017). beta-arrestin1-mediated acetylation of Gli1 regulates Hedgehog/Gli signaling and modulates self-renewal of SHH medulloblastoma cancer stem cells. *BMC Cancer* 17: 488.
- Mirza AN, McKellar SA, Urman NM, Brown AS, Hollmig T, Aasi SZ, *et al.* (2019). LAP2 Proteins Chaperone GLI1 Movement between the Lamina and Chromatin to Regulate Transcription. *Cell* 176: 198-212 e115.
- Nye MD, Almada LL, Fernandez-Barrena MG, Marks DL, ElSawa SF, Vrabel A, *et al.* (2014). The transcription factor GLI1 interacts with SMAD proteins to modulate transforming growth factor beta-induced gene expression in a p300/CREB-binding protein-associated factor (PCAF)-dependent manner. *J Biol Chem* 289: 15495-15506.
- Park KC, Park JH, Jeon JY, Kim SY, Kim JM, Lim CY, *et al.* (2014). A new histone deacetylase inhibitor improves liver fibrosis in BDL rats through suppression of hepatic stellate cells. *Br J Pharmacol* 171: 4820-4830.
- Seki E (2016). HEDGEHOG Signal in hepatocytes mediates macrophage recruitment: A new mechanism and potential therapeutic target for fatty liver disease. *Hepatology* 63: 1071-1073.
- Soares MB, Brustolim D, Santos LA, Bellintani MC, Paiva FP, Ribeiro YM, *et al.* (2006). Physalins B, F and G, seco-steroids purified from *Physalis angulata* L., inhibit lymphocyte function and allogeneic transplant

rejection. *Int Immunopharmacol* 6: 408-414.

Tan S, Liu H, Ke B, Jiang J, & Wu B (2020). The peripheral CB1 receptor antagonist JD5037 attenuates liver fibrosis via a CB1 receptor/beta-arrestin1/Akt pathway. *Br J Pharmacol* 177:2830-2847.

Vandenbergh I, Creancier L, Vispe S, Annereau JP, Barret JM, Pouny I, *et al.* (2008). Physalin B, a novel inhibitor of the ubiquitin-proteasome pathway, triggers NOXA-associated apoptosis. *Biochem Pharmacol* 76: 453-462.

Vidak S, Kubben N, Dechat T, & Foisner R (2015). Proliferation of progeria cells is enhanced by lamina-associated polypeptide 2 alpha (LAP2 alpha) through expression of extracellular matrix proteins. *Gene Dev* 29: 2022-2036.

Wu X, Wu X, Ma Y, Shao F, Tan Y, Tan T, *et al.* (2016). CUG-binding protein 1 regulates HSC activation and liver fibrogenesis. *Nat Commun* 7: 13498.

Yang Y, Yi L, Wang Q, Xie B, Sha C, & Dong Y (2018). Physalin B Suppresses Inflammatory Response to Lipopolysaccharide in RAW264.7 Cells by Inhibiting NF- $\kappa$ B Signaling. *Journal of Chemistry* 2018: 1-6.

Zhang F, Hao M, Jin H, Yao Z, Lian N, Wu L, *et al.* (2017). Canonical hedgehog signalling regulates hepatic stellate cell-mediated angiogenesis in liver fibrosis. *Br J Pharmacol* 174: 409-423.

Zhang F, Wang F, He J, Lian N, Wang Z, Shao J, *et al.* (2020). Reregulation of hepatic stellate cell contraction and cirrhotic portal hypertension by Wnt/beta-catenin signaling via interaction with Gli1. *Br J Pharmacol*.

Zhao SS, Wang JX, Wang YC, Shao RG, & He HW (2015). [Establishment and application of a high-throughput drug screening model based on COL1A1 promoter for anti-liver fibrosis]. *Yao Xue Xue Bao* 50:169-173.

Zheng Y, Chen J, Liu L, Liang X, & Hong D (2016). In vivo pharmacokinetics of and tissue distribution study of physalin B after intravenous administration in rats by liquid chromatography with tandem mass spectrometry. *Biomed Chromatogr* 30: 1278-1284.

Zheng Y, Luan L, Chen Y, Ren Y, & Wu Y (2012). Characterization of physalins and fingerprint analysis for the quality evaluation of *Physalis alkekengi* L. var. *franchetii* by ultra-performance liquid chromatography combined with diode array detection and electrospray ionization tandem mass spectrometry. *J Pharm Biomed Anal* 71:54-62.

Zupkovitz G, Tischler J, Posch M, Sadzak I, Ramsauer K, Egger G, *et al.* (2006). Negative and positive regulation of gene expression by mouse histone deacetylase 1. *Mol Cell Biol* 26: 7913-7928.

## Figure legends

**FIGURE 1** PB inhibits the proliferation and activation of HSCs. (A) The chemical structure of PB. (B-F) LX-2 cells were treated with 2 ng·ml<sup>-1</sup> TGF $\beta$ 1 with or without different concentrations of PB for 24 hr after no FBS starvation. (B) COL1A1 luciferase activity was determined in LX-2 cells transfected with the pGL4.17-COL1A1 luciferase construct. (C) Cell proliferation was determined by CCK8 assay. (D) PB repressed the *COL1A1*,  *$\alpha$ SMA*, *TGF $\beta$ 1* and *TIMP1* in a dose-dependent manner in LX-2 cells. *GADPH* served as loading control. (E) PB dose-dependently inhibited the protein levels of COL1A1 and  $\alpha$ -SMA in LX-2 cells. The protein levels were normalized against  $\beta$ -actin. (F) Immunofluorescence staining for  $\alpha$ -SMA (red) in LX-2 cells. (G-I) Mouse pHSCs were treated with different concentrations of PB for 24 hr after 7 days of isolation. (G) PB inhibited the *col1a1*, *av $\delta$*   *$\alpha$ sma* in mouse pHSCs.  *$\beta$ -actin* served as loading control. (H) PB inhibited the protein levels of  $\alpha$ -SMA in mouse pHSCs. The protein levels were normalized against  $\beta$ -actin. (I) Immunofluorescence staining for  $\alpha$ -SMA (red) in mouse pHSCs. The values are expressed as the mean  $\pm$  SEM of five independent assays, \*P < 0.05, \*\*P < 0.01, \*\*\*P < 0.001, \*\*\*\*P < 0.0001, significantly different from the control group and #P < 0.05, ##P < 0.01, ###P < 0.001 significantly different from the TGF $\beta$ 1 treatment group in LX-2 cells and mouse pHSCs. ns, not significant.

**FIGURE 2** PB markedly ameliorated the liver fibrosis in CCl<sub>4</sub>-treated mice. (A) Liver histopathology was observed by H&E staining (magnification 200×). (B) Serum ALT, AST assays and (C) Liver hydroxyproline concentration assays demonstrated that PB reduced liver fibrosis in CCl<sub>4</sub> mice. (D) The obtained liver sections were subjected to sirius red staining (magnification 200×; up panel), and Masson trichrome stain (magnification 200×; down panel). (E) mRNA expressions of *αSMA*, *Col1a1*, *Tgfb1*, and *Timp1* in mice liver samples. (F) Western blot analysis and semi-quantitation of  $\alpha$ -SMA expressions.  $\beta$ -actin served as the loading control. The values are expressed as the mean  $\pm$  SEM (n = 8 of each group), \*P < 0.05, \*\*P < 0.01, \*\*\*P < 0.001, significantly different from control group and ###P < 0.001, ####P < 0.0001, significantly different from CCl<sub>4</sub>-corn oil group. ns, not significant.

**FIGURE 3** PB markedly ameliorated the liver fibrosis in bile duct-ligated (BDL) mice. (A) Liver pathological changes were detected by H&E staining (magnification 200x). (B) Serum ALT, AST assays and (C) Liver hydroxyproline concentration assays demonstrated that PB reduced liver fibrosis in BDL mice. (D) The degree of liver collagen accumulation was determined by sirius red staining (magnification 200x; up panel), and Masson trichrome stain (magnification 200x; down panel). (E) mRNA expressions of *αSMA*, *Col1a1*, *Tgfb1*, and *Timp1* in mice liver sample. (F) Western blot analysis and semi-quantitation of  $\alpha$ -SMA expressions.  $\beta$ -actin served as the loading control. The values are expressed as the mean  $\pm$  SEM (n = 8 of each group), \*P < 0.05, \*\*P < 0.01, \*\*\*P < 0.001, significantly different from control group and ###P < 0.001, ####P < 0.0001, significantly different from BDL group. ns, not significant.

**FIGURE 4** PB suppressed the GLI1 expression *in vitro* and *in vivo*. (A) PB repressed GLI-luciferase activities. (B-C) PB administration down-regulated GLI1(B) mRNA and (C) protein expressions in LX-2 cells. *GADPH* / $\beta$ -actin served as loading control. (D-E) PB administration down-regulated GLI1 mRNA(D) and (E) protein expressions in mouse pHSCs. *β-actin* / $\beta$ -actin served as loading control. (F) PB administration down-regulated GLI1 protein expressions in BDL livers.  $\beta$ -actin served as loading control. The *in vitro* values are expressed as the mean  $\pm$  SEM of five independent assays, \*P < 0.05, \*\*P < 0.01, \*\*\*P < 0.001, significantly different from the control group, #P < 0.05, ###P < 0.001 significantly different from the TGF $\beta$ 1 treatment group in LX-2 cells. The *in vivo* values are expressed as the mean  $\pm$  SEM (n = 8 of each group), #P < 0.05; significantly different from sham group, \*P < 0.05; significantly different from BDL-NS group. ns, not significant.

**FIGURE 5** Altering GLI1 expression influenced the antifibrotic activity of PB. (A-B) LX-2 cells were transfected with 100 nM GLI1 siRNA1/2 or Ctrl siRNA (A) the mRNA expressions of fibrogenic gene were analyzed by RT-qPCR. *GADPH* served as loading control. (B) Western blot analysis and semi-quantitation of GLI1,  $\alpha$ -SMA and Collagen  $\alpha$ 1(I) expressions.  $\beta$ -actin served as the loading control. (C) LX-2 cells were transfected with 100 nM GLI1 siRNA1/2 or Ctrl siRNA and subsequently treated with 2 ng·ml<sup>-1</sup> TGF $\beta$ 1 with or without different concentrations of PB for 24 hr after no FBS starvation. The same protein expressions were detected by western blot with the indicated antibodies.  $\beta$ -actin was used as a loading control for all western blot assays. LX-2 cells were transfected with (D) 2.5- $\mu$ g HA-GLI1 or vector for 6 hr and subsequently treated with 2 ng·ml<sup>-1</sup> TGF $\beta$ 1 with or without different concentrations of PB for 24 hr after no FBS starvation. The protein expressions of HA and liver fibrosis markers were determined by immunoblotting with the indicated antibodies. The data are expressed as the mean  $\pm$  SEM of five independent assays, \*P < 0.05, \*\*P < 0.01, \*\*\*P < 0.001, significantly different from the Ctrl siRNA group, #P < 0.05, ##P < 0.01, ###P < 0.001, significantly different from the pcDNA /Ctrl siRNA group +TGF $\beta$ 1 group, <sup>P</sup> < 0.05, significantly different from the pcDNA + TGF $\beta$ 1 + PB1 - mM group.

**FIGURE 6** PB blocked the nuclear localization of GLI1 in HSCs. (A) The nuclear and cytoplasmic extractions of LX-2 cells were separated after PB treatment and analysed by western blot. (B) LX-2 cells and (C) mouse pHSCs in dishes were fixed in 4% paraformaldehyde, stained with DAPI (blue) and GLI1 (red), and imaged by confocal microscopy, Scale bar: 20  $\mu$ m. (D-E) The mRNA expressions of the GLI1 downstream genes *HHIP*, *CYCLIN D*, *CYCLIN E* and *C-MYC* (D) in LX-2 cells and (E) in BDL group. The values are expressed as the mean  $\pm$  SEM of five independent assays, \*P < 0.05, \*\*P < 0.01, \*\*\*P < 0.001, significantly different from the control group, #P < 0.05, ###P < 0.001, significantly different from

the TGF $\beta$ 1 treatment group. ns, not significant.

**FIGURE 7** PB interrupted the LAP2 $\alpha$ /HDAC1 complex. (A) HA-GLI1 was transfected into HEK293T cells. Whole cell extracts were immunoprecipitated with an anti-HA antibody. (B) Western blot analysis of GLI1, LAP2 $\alpha$  and HDAC1 expression in LX-2 cells.  $\beta$ -actin served as a loading control. (C) Myc-LAP2 $\alpha$  and HA-GLI1 were transfected into HEK293T cells. The interaction between Myc-LAP2 $\alpha$  and HA-GLI1 was investigated using immunoprecipitation assays. (D) Myc-LAP2 $\alpha$  and FLAG-HDAC1 were transfected into HEK293T cells. The interaction between Myc-LAP2 $\alpha$  and FLAG-HDAC1 was investigated using immunoprecipitation assays. The interaction between LAP2 $\alpha$  and HDAC1 was investigated using immunoprecipitation assays in LX-2 cells (E) and (F) CCl<sub>4</sub>-mice (G) LX-2 cells in dishes were fixed in 4% paraformaldehyde, stained with DAPI (blue), LAP2 $\alpha$  (green) and HDAC1 (red) and imaged by confocal microscopy, Scale bar: 20  $\mu$ m. The values are expressed as the mean  $\pm$  SEM of five independent assay.

**FIGURE 8** LAP2 $\alpha$  and HDAC1 were of significance to the antifibrotic effects of PB. (A-C) LX-2 cells treated with PB (1  $\mu$ M) and/or Vorinostat (10  $\mu$ M, 6 hr) then (A) the protein expressions of GLI1 and fibrogenic markers were detected by immunoblotting with the indicated antibodies and (B) the protein expressions of GLI1 were detected by immunofluorescence staining. (C) HEK293T cells was transfected with HA-GLI1 and/or treated with PB (1  $\mu$ M) or Vorinostat (10  $\mu$ M, 6 hr), Whole cell extracts were immunoprecipitated with an anti-HA antibody. (D-G) 100-nM LAP2 $\alpha$ -1/2 siRNA or Ctrl siRNA 48 hr. (D) The fibrotic mRNA and (E) protein expressions were detected by western blot and RT-qPCR. (F) The protein expressions of GLI1 were detected by immunofluorescence staining. (G) HEK293T cells was transfected with HA-GLI1 and/or treated with PB (1  $\mu$ M) or si-LAP2 $\alpha$ , Whole cell extracts were immunoprecipitated with an anti-HA antibody. The values are expressed as the mean  $\pm$  SEM of five independent assays, \*P < 0.05, \*\*P < 0.01, \*\*\*P < 0.001, significantly different from the control group.

**FIGURE 9** Physalin B (PB) disrupted the interaction between LAP2 $\alpha$  and HDAC1, which enhanced the effect of GLI1 acetylation. The increase of GLI1 acetylation further inhibited GLI1 exerting effect on liver fibrosis.

Figure 1

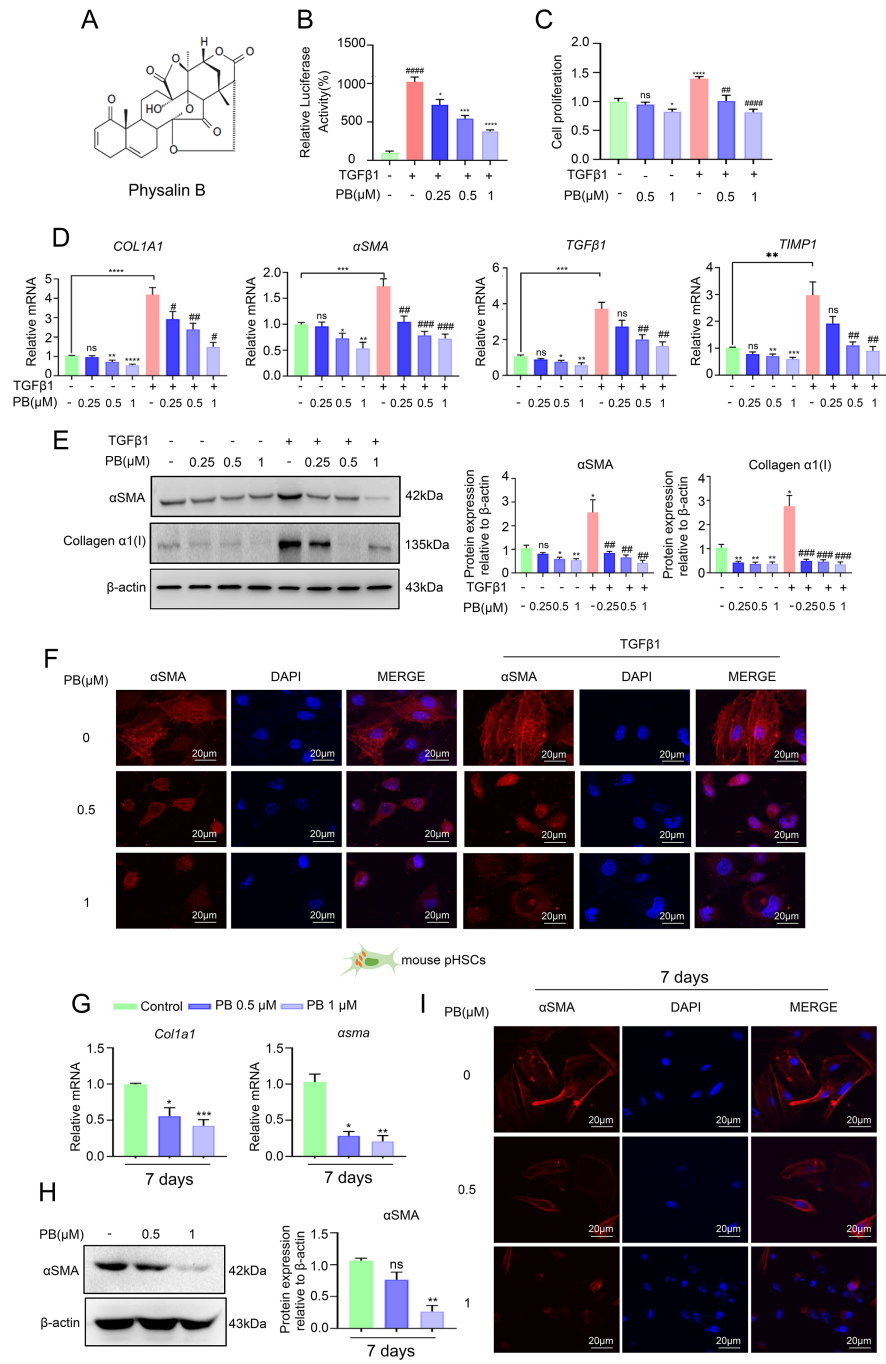


Figure 2

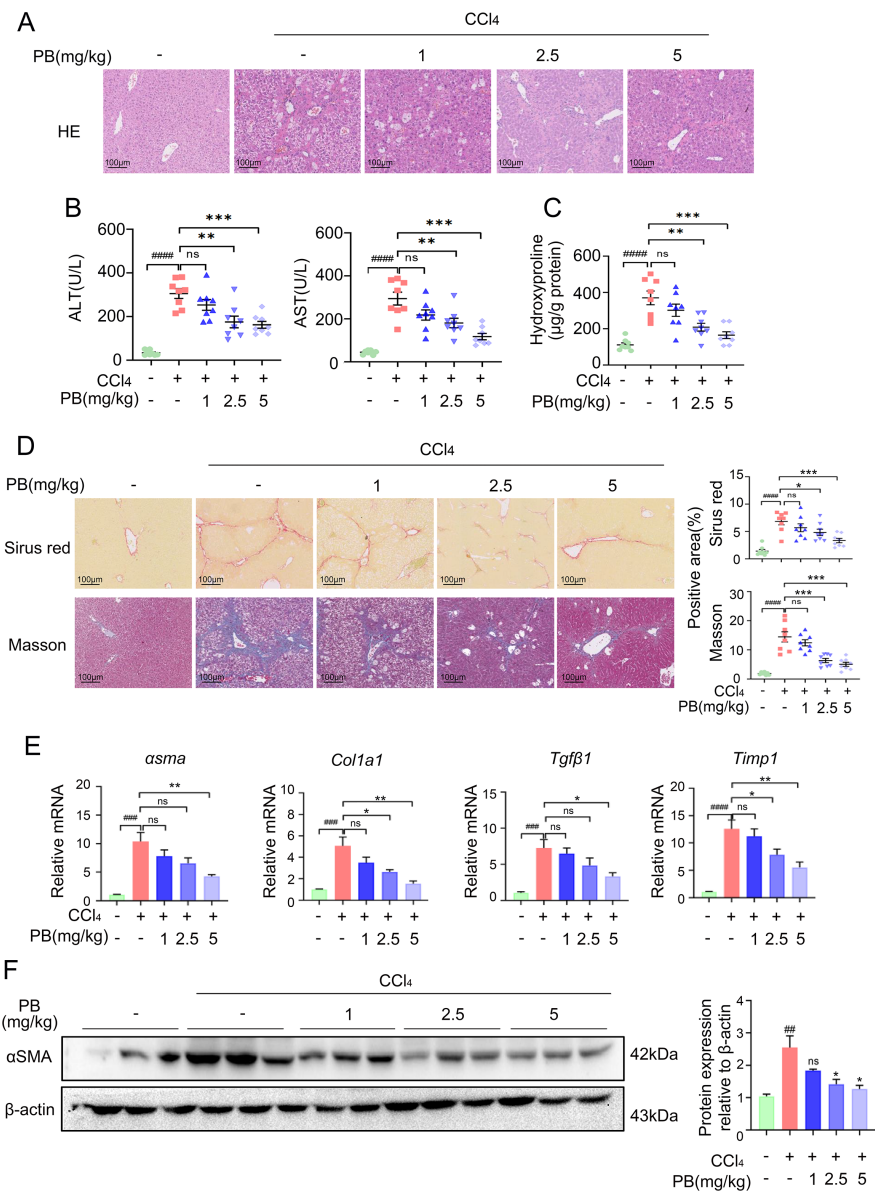


Figure 3

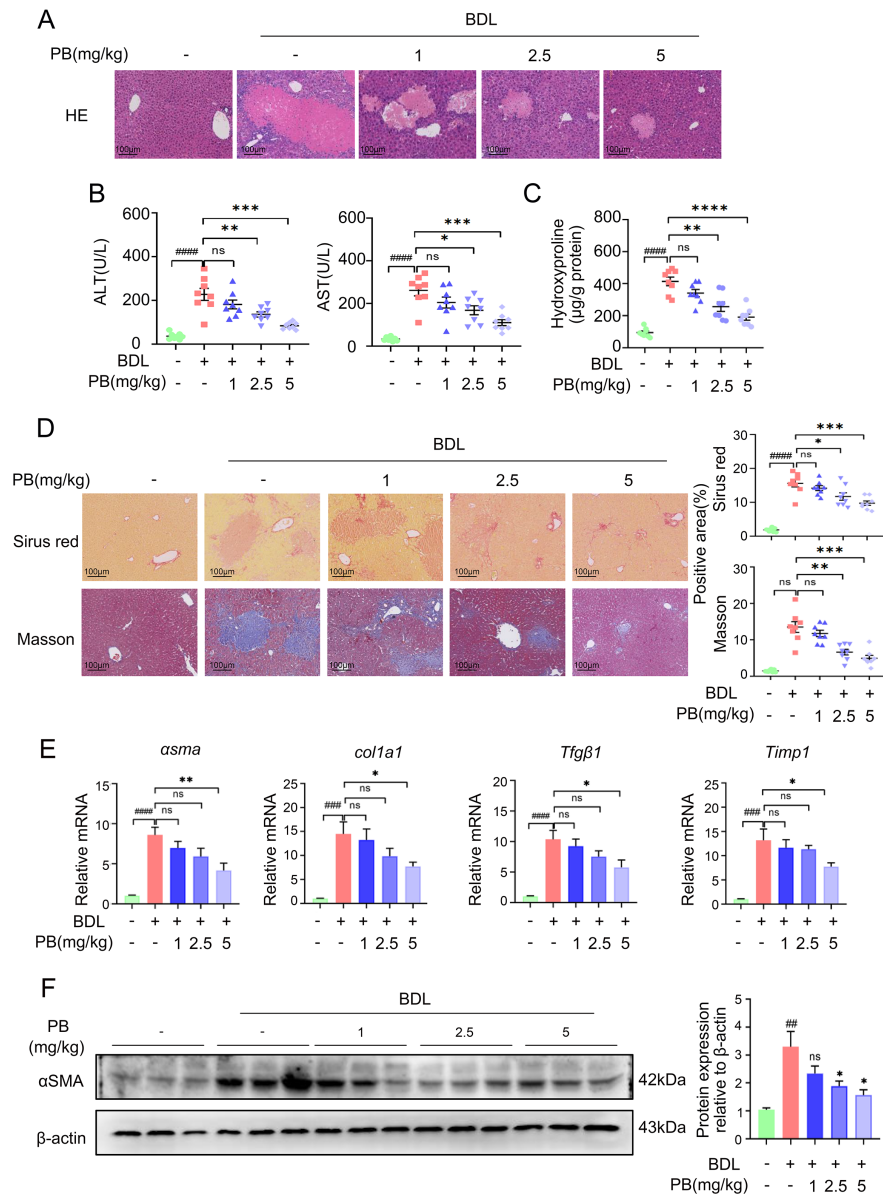


Figure 4

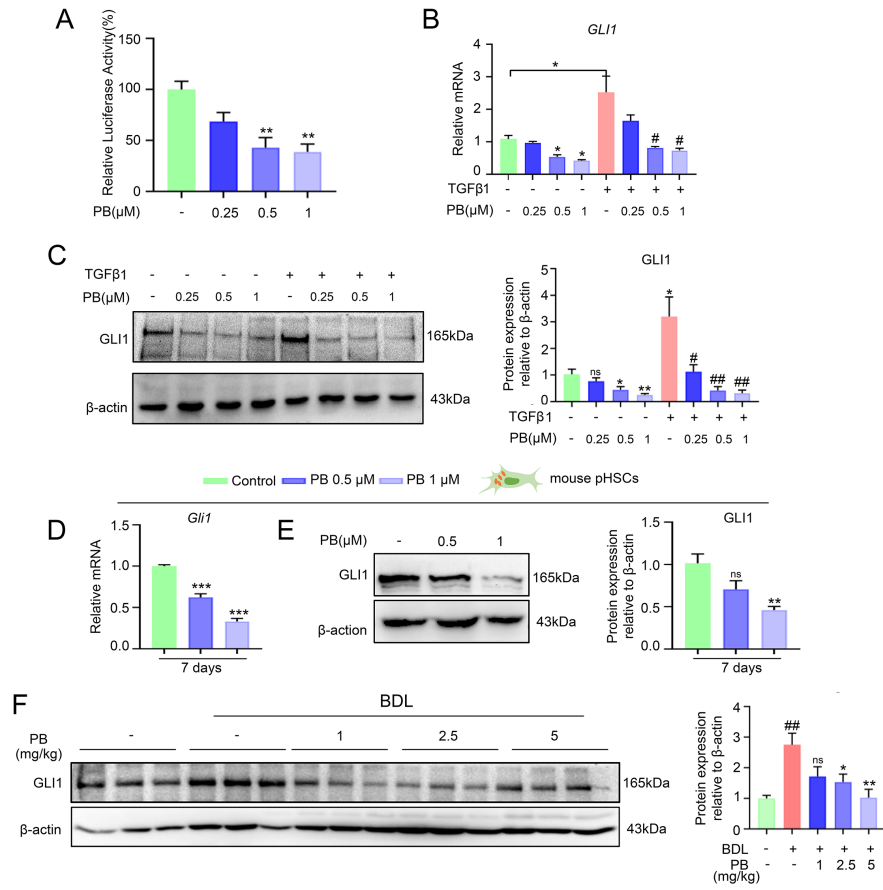


Figure 5

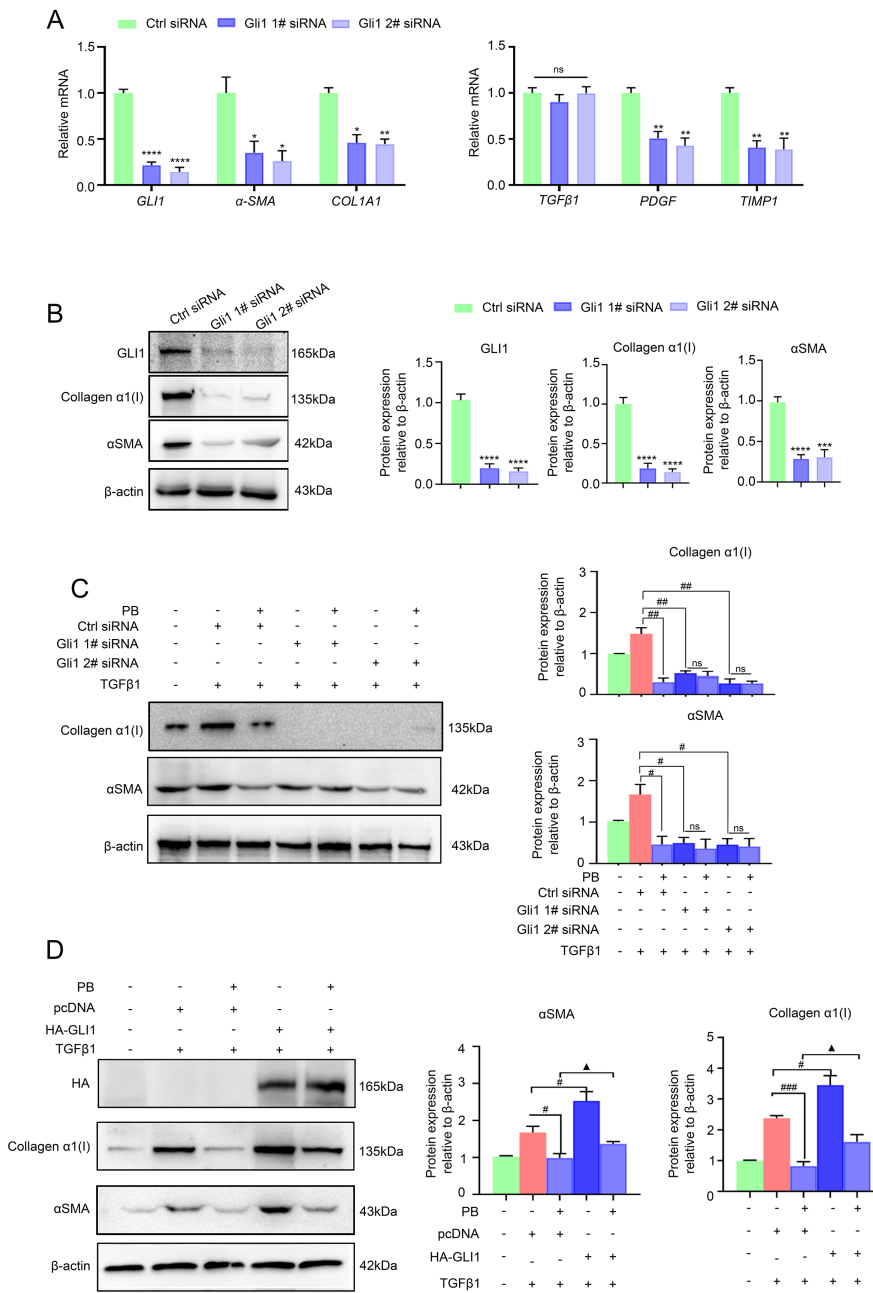


Figure 6

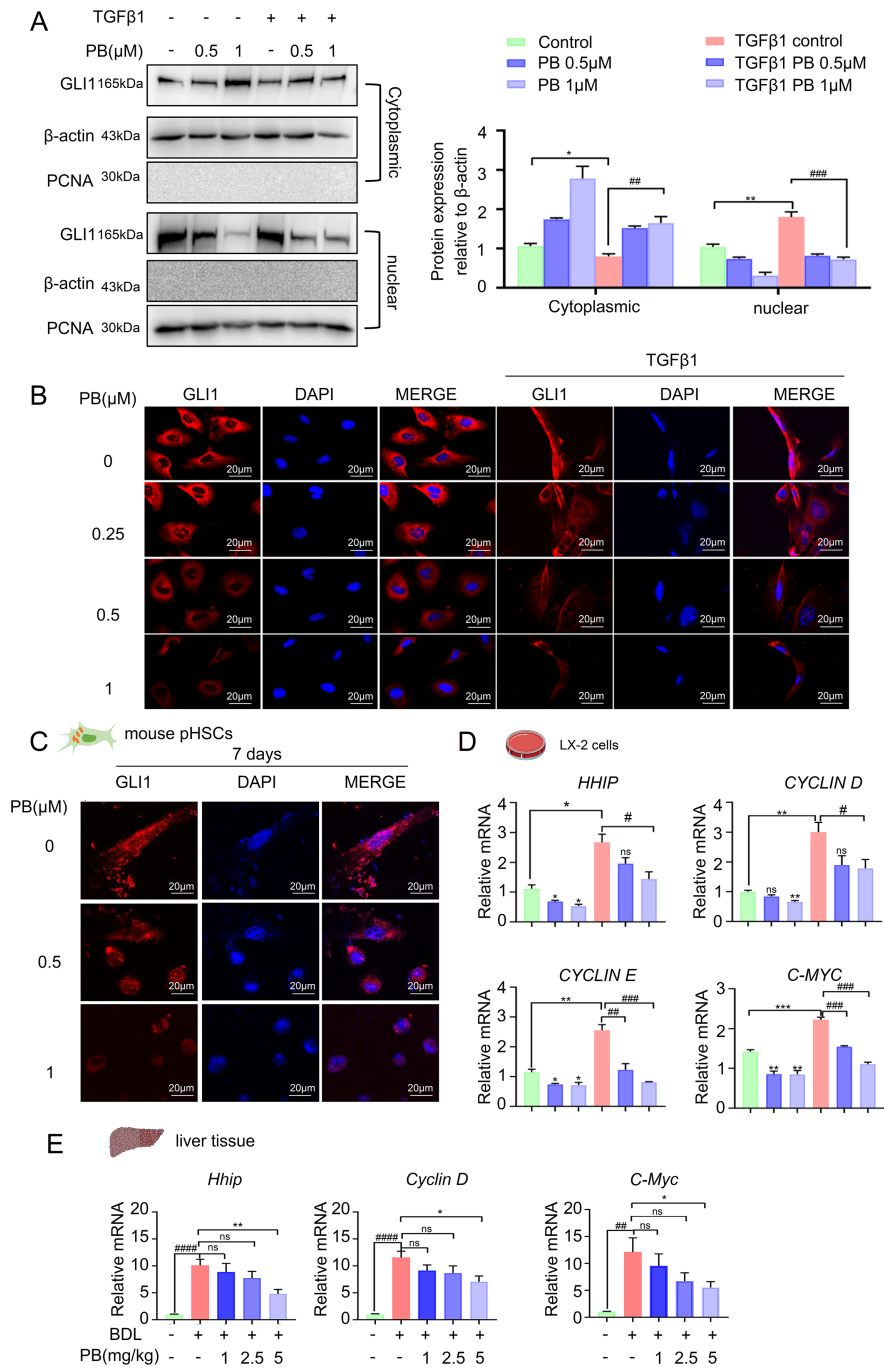


Figure 7

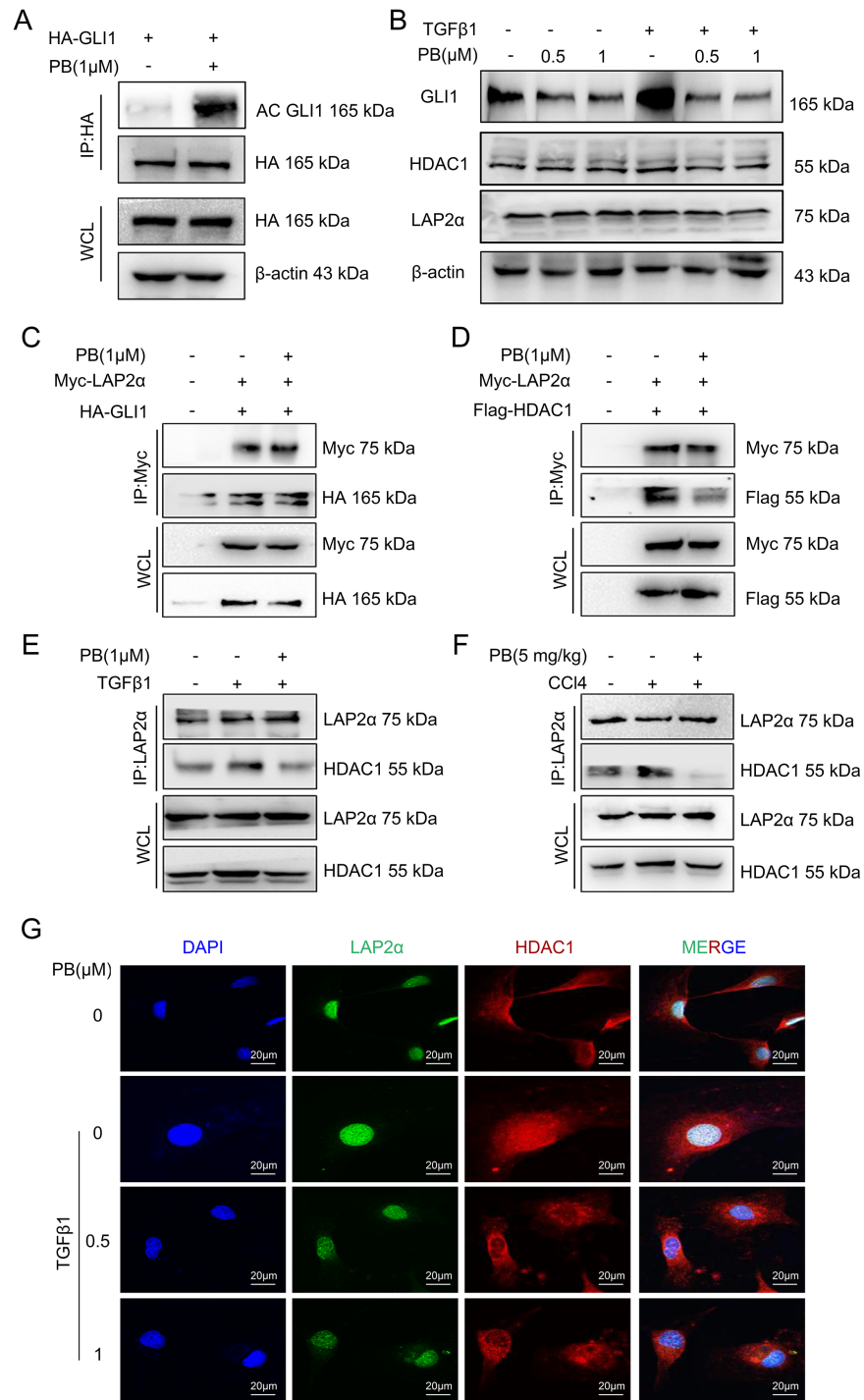


Figure 8

